

Boundary effects in the TASEP model

MSc Thesis, 25.6.2018

Author:

EINO MARTTI ILMARI ELO

Supervisor:

JUHA MERIKOSKI



UNIVERSITY OF JYVÄSKYLÄ
DEPARTMENT OF PHYSICS

© 2018 Eino Martti Ilmari Elo

Julkaisu on tekijänoikeussäännösten alainen. Teosta voi lukea ja tulostaa henkilökohtaista käyttöä varten. Käyttö kaupallisiin tarkoituksiin on kielletty. This publication is copyrighted. You may download, display and print it for Your own personal use. Commercial use is prohibited.

Tiivistelmä

Asymmetrinen eksklusioprosessi on keskeinen malli poissa tasapainosta tapahtuville siirtoprosesseille. Vertaan tässä tutkielmassa normaalia TASEP-mallia (totally asymmetric exclusion process) kahteen uuteen malliin, joissa on erilaiset reunaehdot systeemin etureunassa. Yhdessä mallissa hiukkaset saapuvat systeemiin pareittain. Toisessa mallissa hiukkasten systeemiintulotaajuus riippuu siitä, onko toisessa hilapaikassa hiukkanen vai ei.

Näiden mallien tarkoituksena on reunailmiöiden tutkiminen. Käyttämäni menetelmät ovat matriisiyrite, keskimääräisen kentän approksimaatio, kineettinen jatkuvan ajan Monte Carlo -simulaatio ja master-yhtälöiden symbolinen ja numeerinen ratkaiseminen.

Saavutetuista tuloksista mielenkiintoisin on se, että mallien tiheysprofiilit ja tiheyden todennäköisyystiheydet saadaan hyvänä approksimaationa vastaamaan tavallista TASEPia, jossa hiukkasilla on tietty keskimääräisen kentän approksimaation ennustama sisääntulotaajuus. Matalan tiheyden faasissa sekä matalan ja korkean tiheyden faasien koeksistenssiviivalla tämä tosin ei toimi kovin hyvin.

Abstract

The asymmetric exclusion process is the quintessential model of non-equilibrium transport phenomena. In this graduate thesis I compare TASEP (totally asymmetric exclusion process) to two new models that have a different behavior at the right edge of the system. In one model particles enter the system two at a time filling the two leftmost lattice sites. In the other one particles enter the system with different rates depending on whether the second lattice site is occupied or not.

The aim in creating these models is to study boundary effects. Techniques I use to this end are the matrix ansatz method, mean field theory, domain-wall theory, continuous time kinetic Monte Carlo simulations and solving the Master equations exactly for small systems symbolically and numerically.

The most interesting result is that the density profiles and the probability density profiles of the average densities have a close correspondence with those of normal TASEP that has a certain entry frequency anticipated by mean field theory. For small density phase this works less well.

Contents

1	Introduction	7
1.1	Non-equilibrium systems	7
1.2	TASEP and this thesis	8
2	Models	11
3	What is known about the usual open TASEP?	13
4	Methods	15
4.1	Direct analytical solution	15
4.2	Exact numerics	16
4.3	Monte Carlo simulation	17
4.4	Analytical solution by matrix ansatz	17
4.5	Mean Field Theory	20
4.5.1	Model 1	20
4.5.2	Model 2	21
4.5.3	Model 3	22
4.6	Domain Wall Theory	22
5	Results	25
6	Conclusion	35
	References	37

1 Introduction

1.1 Non-equilibrium systems

What is the behavior of systems consisting of large numbers of particles like? Ludwig Boltzmann made good progress on this question in 1870s by postulating that eventually isolated systems stop evolving and all microstates become equally probable, a state of affairs called equilibrium. This is all fine and good but what about open systems and systems that have not yet reached equilibrium?

As an example of such a system consider a tube connecting two infinite particle reservoirs held at different chemical potentials. Particles will irreversibly flow through the tube towards lower chemical potential at some nearly constant rate. Clearly the system is not at equilibrium, but beside some fluctuations the properties of the system do not change with time. This state of affairs is called a (non-equilibrium) steady state.

Non-equilibrium systems near equilibrium have been understood relatively well since the middle of 20th century thanks to researchers like Onsager and Kubo,^[1,2] but what their results boil down to is just a perturbation scheme around the equilibrium. These results are not useful far from equilibrium.

Non-equilibrium systems do not have underlying Hamiltonians H (since energy enters and leaves the system) or partition functions Z (since they do not have Hamiltonians) and they do not have a well-defined temperature T (since the zeroth law of thermodynamics is not applicable). Since this is the case, it is obviously not possible to generate the probability density function ρ with the equilibrium statistical mechanics trick leading to the Boltzmann-Gibbs law $\rho = e^{-H/kT}/Z$.

There is currently no known general description for the macroscopic state of a non-equilibrium system. It is not even known what parameters could be used to derive one. At this stage a lot of research goes into simple models of non-equilibrium physics hoping that there are generalizable lessons to learn.

Detailed balance does not hold for all NE systems. This means that instead of the evolution of the system stopping as time goes on (probability currents going to zero), there is a constant current. This is reminiscent of magneto-statics as opposed to electrostatics.

1.2 TASEP and this thesis

Driven lattice gas models are a class of models of non-equilibrium transport phenomena. The asymmetric simple exclusion process (ASEP) is a particularly simple such model. In ASEP particles undergo biased (hence asymmetric) diffusion and interact with hard-core repulsion (meaning that particles can only move to unoccupied cells, hence exclusion) making it a genuine many-body problem. The word process signifies the fact that ASEP is a kinetic theory and lacks a Hamiltonian. Due to its simplicity it has become the paradigmatic model for describing transport phenomena. The role of ASEP in non-equilibrium physics is similar to that of the Ising model in equilibrium physics.^[3]

ASEP was originally conceived of in 1968 as a model for the motion of ribosomes along m-RNA molecules as they are translated to proteins.^[4] ASEP has been studied with periodic boundary conditions e.g. in a ring geometry, (as is obvious from looking at the figure 1b for a few seconds, it has uniform density measure) and also with multiple classes of particles, each overtaking particles of the lower classes. ASEP has a mapping to an interface problem (just replace particles with downward slopes and holes with upward slopes). For an pretty illustration all of this see figure 1.

Pertaining to the original biological application of ASEP; Chou, Mallick and Zia have written a good review of ASEP in biological transport.^[5] ASEP has also been used as a model for road traffic,^[6,7] bio-polymerization and the movement of DNA along a matrix in gel electrophoresis,^[8,9] pedestrian dynamics^[10] and current in zeolites.^[11]

Real systems have boundaries and they sometimes have important consequences deep within the systems. One motivation for this study has been boundary effects in a propagating one dimensional interface,^[12] see figure 1d for the mapping of ASEP to interface dynamics.

In this thesis I introduce two models meant to probe the boundary effects of TASEP, the totally asymmetric exclusion process. TASEP is a slight simplification of ASEP, where particles are only allowed to move in one direction, so it is totally asymmetric.

Normally particles enter TASEP from its leftmost lattice site at some rate α whenever that lattice site is empty. In one of my models particles are introduced into the system in pairs, filling the two first lattice sites. In the other model particles enter the leftmost lattice site of the system with different rates, depending on whether the second lattice site is empty or filled.

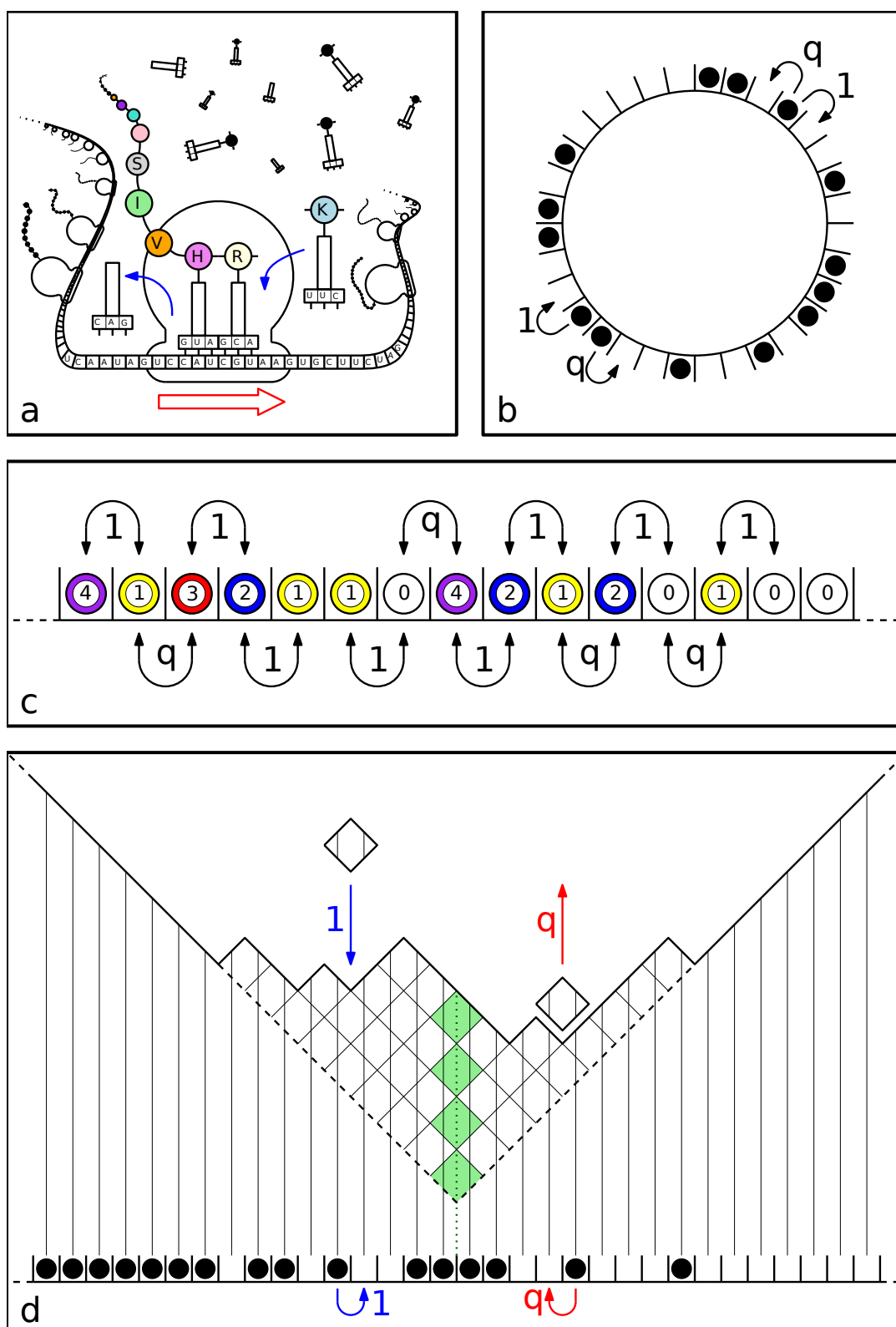


Figure 1. The ASEP's family album: a) Ribosomes on mRNA, b) Periodic ASEP, c) Multispecies ASEP, d) Surface growth. Image from Alexandre Lazarescu, *The Physicist's Companion to Current Fluctuations: One-Dimensional Bulk-Driven Lattice Gases*

2 Models

TASEP is set in a one-dimensional lattice of length L . Each lattice site k is either empty or occupied by a particle. A nice representation is that using binary strings $n = (n_1 \dots n_L)$, where $n_k = 1$ for occupied sites and $n_k = 0$ for empty sites.

Boundary conditions are open with particles entering from the left with entry rate α and leaving one at a time from the right with exit rate β . The particles jump to the right at rate 1. Particles only jump forwards or enter the system when there are no particles at the lattice site they would end up at. See figure 2 for an illustration.

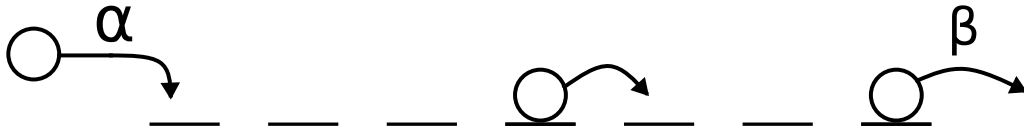


Figure 2. Particles randomly enter the system from one side at rate α , jump forwards if there is an opening at rate 1 and exit the system from the other end at rate β . This is the standard TASEP or model 1.

In model 2 particles enter the lattice in pairs as illustrated in figure 3. Model 3 has different entry rate depending on whether the second lattice site is filled or empty as illustrated in figure 4.

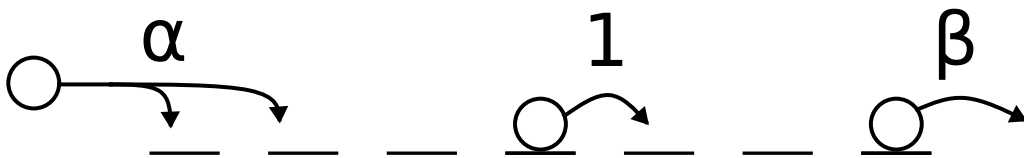


Figure 3. In model 2 particles enter the system in pairs.



Figure 4. In model 3 particles enter the system with a different rate depending on whether lattice site 2 is occupied or not.

Another possibly interesting model would have α depend on time, $\alpha = \alpha(t)$. We could have for example a gate that flips α between 0 and α_0 . For stochastic flipping mean field theory could be utilized, but for deterministic flipping there seems to not exist an approximation scheme like that. For very fast flipping mean field theory still works well, however.

Since these systems are Markovian, their steady-state weights can be formally obtained directly from the rules governing their evolution, as is shown in chapter 4.1 for model 1. Since this method requires solving a system of 2^L equations, it is not useful for numerical work on large systems.

3 What is known about the usual open TASEP?

The vector containing the exact average occupation numbers at steady state (more succinctly the stationary measure) was solved for TASEP in 1992 by Derrida et. al.^[13] by using recursion relations. In 1993 Derrida and Evans calculated all the moments of the density profile of ASEP.^[14] Later the same year Derrida et al. presented a solution for ASEP using a matrix product formulation.^[15] This method is reviewed in^[16]. The phase diagram in the $L \rightarrow \infty$ limit is shown in figure 5.

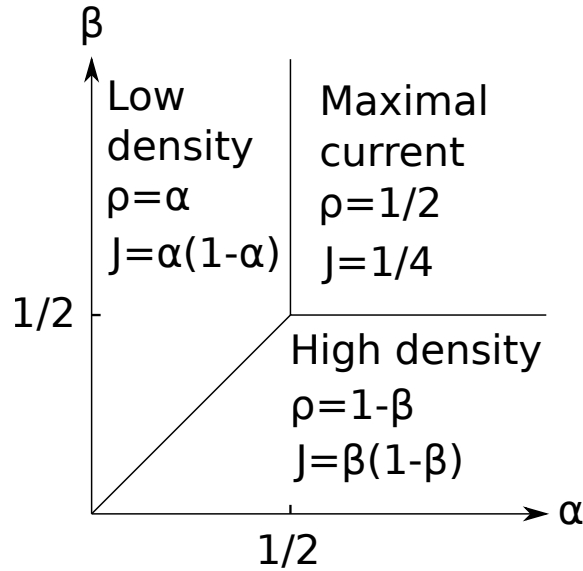


Figure 5. Phase diagram for the standard TASEP or model 1 in the limit $L \rightarrow \infty$. The line at $\alpha = \beta$ is of the first order and the lines $\alpha = 1/2$ and $\beta = 1/2$ are of the second order

For a system of size L the stationary measure for TASEP densities is

$$\begin{aligned}
 \langle n_k \rangle_L &= \sum_{p=0}^{L-k-1} \frac{\langle W | C^{L-p-1} | V \rangle}{\langle W | C^L | V \rangle} + \frac{\langle W | C^{k-1} | V \rangle}{\langle W | C^L | V \rangle} \sum_{p=2}^{L-k+1} \frac{(p-1)(2L-2k-p)!}{(L-k)!(L-k-p+1)!} \beta^{-p} \\
 \langle n_L \rangle_L &= \frac{\langle W | C^{L-1} | V \rangle}{\beta \langle W | C^L | V \rangle}
 \end{aligned} \tag{1}$$

where n_k is the occupation number of the k :th lattice site and

$$\langle W | C^L | V \rangle = \sum_{p=1}^L \frac{p(2L-1-p)!}{L!(L-p)!} \frac{(1/\beta)^{p+1} - (1/\alpha)^{p+1}}{(1/\beta) - (1/\alpha)}. \quad (2)$$

I shall properly explain the matrix and vectors in chapter 4.4. Matrix C is defined using the matrices in that chapter as $C = D + E$, where an occupied lattice site is encoded as D and an empty site as E .

Current through the system is obviously the likelihood that the last lattice site is occupied multiplied by the rate at which the particles leave that site, $\langle n_L \rangle * \beta$. From equation (1) we thus gain

$$J_L = \frac{\langle W | C^{L-1} | V \rangle}{\langle W | C^L | V \rangle}. \quad (3)$$

On the other hand, the current in the bulk of the system is

$$J = \langle n_k(1 + n_{k+1}) \rangle = \langle n_k \rangle + \langle n_k n_{k+1} \rangle, \quad (4)$$

so that the correlation between adjacent cells can be gained from the density $\langle n_k \rangle$ by subtracting the current, which is just β times the density at the last cell. This also works for model 2 except for the first two lattice points.

The exact statistics of the current for ASEP with open boundaries were found by A. Lazarescu and K. Mallick in 2011^[17]. Their methods are reviewed in Lazarescu 2015^[18].

4 Methods

In this chapter we review some of the methods used in the literature for the usual TASEP and discuss their use for models 2 and 3.

4.1 Direct analytical solution

An example of a configuration for a system of size $L = 4$ would be $(0,0,1,0)$, where the first, second and fourth sites are empty and the third site is occupied.

After a bit of examination it should be apparent that in steady state the following system of equations holds for systems of size 3 in the case of model 2:

$$\begin{aligned}
 -\alpha P(0,0,0) + \beta P(0,0,1) &= 0, \\
 -\alpha P(0,0,1) - \beta P(0,0,1) + P(0,1,0) &= 0, \\
 -P(0,1,0) + \beta P(0,1,1) + P(1,0,0) &= 0, \\
 -\beta P(0,1,1) + P(1,0,1) &= 0, \\
 -P(1,0,0) + \beta P(1,0,1) &= 0, \\
 -P(1,0,1) - \beta P(1,0,1) + P(1,1,0) &= 0, \\
 \alpha P(0,0,0) - P(1,1,0) + \beta P(1,1,1) &= 0, \\
 \alpha P(0,0,1) - \beta P(1,1,1) &= 0.
 \end{aligned} \tag{5}$$

To make it more obvious where these equations come from, here is a way to read the first equation: the probability of the state $(0,0,0)$ increases with rate $\beta P(0,0,1)$ and decreases with rate $-\alpha P(0,0,0)$, and in steady state its time derivative is zero.

The solution of equations (5) as unnormalized probabilities is

$$\begin{aligned}
 P(0,0,0) &= \beta^2(\beta + 1) \\
 P(0,0,1) &= \alpha\beta(\beta + 1) \\
 P(0,1,0) &= \alpha\beta(\beta + 1)(\alpha + \beta) \\
 P(0,1,1) &= \alpha(\alpha + \beta) \\
 P(1,0,0) &= \alpha\beta^2(\alpha + \beta) \\
 P(1,0,1) &= \alpha\beta(\alpha + \beta) \\
 P(1,1,0) &= \alpha\beta(\beta + 1)(\alpha + \beta) \\
 P(1,1,1) &= \alpha^2(\beta + 1).
 \end{aligned} \tag{6}$$

For general L the system of equations is gained by writing

$$\begin{aligned}
& \alpha(n_1 n_2 - (1 - n_1)(1 - n_2))P(0,0 \dots n_L) \\
& + (n_2 - n_1)P(1,0 \dots n_L) \\
& + \dots \\
& + (n_L - n_{L-1})P(n_1 \dots 1,0) \\
& + \beta(1 - 2n_L)P(n_1 \dots 1) = 0
\end{aligned} \tag{7}$$

for all 2^L configurations $(n_1 \dots n_L)$.

Just like Gibbs-Boltzmann distribution in equilibrium physics, this is a probability distribution over the allowed configurations of the system. My implementation of this algorithm in Mathematica got stuck if I tried to solve a system larger than five cells.

Existing recursion relations for model 1 are, if generalized for model 2, very cumbersome apart from special cases.

4.2 Exact numerics

For numerical work, we shall find for all configurations all the other configurations that can be directly reached with allowed processes. For our example configuration of $(0,0,1,0)$ these are $(1,1,1,0)$ with rate α and $(0,0,0,1)$ with rate 1. The transition matrix is formed from these rates by setting $W_{(0,0,1,0),(1,1,1,0)} = \alpha$ and $W_{(0,0,1,0),(0,0,0,1)} = 1$ and so on, and then performing the following transformations

$$\begin{aligned}
W &= W / \max \left(\sum_i W_{i,j} \right) \\
W &= W + I - \sum_j W_{i,j} \\
W &= W^\dagger.
\end{aligned} \tag{8}$$

This results in a matrix $W(i,j)$ where the probability that the system is in configuration i at time $t + dt$, if it was in configuration j at time t .

The steady state is the dominant eigenvector of this matrix. This method relies on the non-negativity of all the rates and follows from the Perron-Frobenius theorem.

This is pretty much just a different way of doing what was done in last chapter, with 2^L equations traded for a 2^L times 2^L matrix. My implementation of this algorithm in Matlab solves a system of size 16 in 1 second.

As an aside, the rate $W(010,100)$ and probabilities $P(100)$ and $P(010)$ are obviously positive but $W(100,010)$ is obviously zero, so detailed balance^[19]

$$P_{\{n\}} W(\{n\} \rightarrow \{m\}) = P_{\{m\}} W(\{m\} \rightarrow \{n\}) \tag{9}$$

is indeed broken.

4.3 Monte Carlo simulation

Continuous time Monte Carlo simulations are done using the Gillespie algorithm.^[20] It uses time steps of $dt = \log(1/r)/Q$, where r is a random number from $(0,1]$ and Q is the sum of rates of possible processes. For our example configuration $(0,0,1,0)$, $Q = \alpha + 1$. Using these time steps allows a direct comparison to exact numerics of chapter 4.2. With Monte Carlo simulations, in principle arbitrarily large systems can be studied, but the computational cost for obtaining reasonably accurate estimates for the observables increases rapidly for increasing L .

The simulation proceeds at each time step by picking a process randomly from the available ones using their rates as weights. For our example configuration this results in $(1,1,1,0)$ α/Q of the time and in $(0,0,0,1)$ $1/Q$ of the time.

4.4 Analytical solution by matrix ansatz

The evolution equation of TASEP is given by^[15]

$$\begin{aligned} \frac{d}{dt}P &= \sum_{\sigma_1} (h_1)_{n_1;\sigma_1} P(\sigma_1, n_2 \dots) \\ &+ \sum_{i=1}^{N-1} \sum_{\sigma_i} h_{n_1, n_2; \sigma_1, \sigma_2} P(n_1 \dots \sigma_i, \sigma_{i+1} \dots n_L) \\ &+ \sum_{\sigma_L} (h_L)_{n_L; \sigma_L} P(\dots n_{L-1}, \sigma_L), \end{aligned} \quad (10)$$

where the matrix elements different from zero for the standard TASEP (model 1) are

$$\begin{aligned} h_{11}(1; 0) &= \alpha, & h_{11}(0; 0) &= -\alpha, \\ h(0, 1; 1, 0) &= 1, & h(1, 0; 1, 0) &= -1, \\ h_L(0; 1) &= \beta, & h_L(1; 1) &= -\beta. \end{aligned} \quad (11)$$

The assumption that

$$\begin{aligned} \sum_{\sigma_1} (h_1)_{n_1; \sigma_1} P_L(\sigma_1, n_2 \dots) &= x_{n_1} P_{L-1}(n_2 \dots) \\ \sum_{\sigma_i} h_{n_1, n_2; \sigma_1, \sigma_2} P_L(\dots n_{i-1}, \sigma_i, \sigma_{i+1}, n_{i+2} \dots) &= -x_{n_i} P_{L-1}(\dots n_{i-1}, n_{i+1}) + x_{n_{i+1}} P_{L-1}(\dots n_i, n_{i+2} \dots) \\ \sum_{\sigma_L} (h_L)_{n_L; \sigma_L} P_L(\dots n_{L-1}, \sigma_L) &= x_{n_L} P_{L-1}(\dots n_{L-1}) \end{aligned} \quad (12)$$

can be rewritten as

$$\begin{aligned}\alpha P_L(0\dots) &= -x_0 P_{L-1}(\dots) = x_1 P_{L-1}(\dots) \\ P_L(\dots 1, 0\dots) &= -x_1 P_{L-1}(\dots 0\dots) + x_0 P(\dots 1\dots) \\ \beta P_L(\dots 0) &= -x_0 P_{L-1}(\dots)\end{aligned}\tag{13}$$

Obviously now $x_1 = -x_0$ and it turns out that the choice $x_1 = -x_0 = 1$ works.

Let us further assume that there exist some vectors V and W and matrices E and D such that the probability of a state is proportional to what is acquired by writing the binary string representing the state, replacing all the zeros with E :s and ones with D :s, and sandwiching the entire thing between V and W , for example $P(0,0,1,0) \propto \langle V | EEDE | W \rangle$. Now the assumption (13) can obviously be rewritten as

$$\begin{aligned}\alpha \langle V | E &= \langle V |, \\ DE &= D + E, \\ \beta D | W \rangle &= | W \rangle.\end{aligned}\tag{14}$$

This results in the correct description of the steady state as proven in^[15].

As a tiny example of the usage of these rules let us solve $P(0,0,1,0)$ up to a normalizing constant.

$$\begin{aligned}P(0,0,1,0) \propto \langle V | EEDE | W \rangle &= \langle V | EED | W \rangle + \langle V | EEE | W \rangle \\ &= \frac{1}{\alpha^2 \beta} + \frac{1}{\alpha^3},\end{aligned}\tag{15}$$

where $DE = D + E$ was used in the intermediate step.

For model 2 the only difference is that instead of h_{11} we use h_{12} , where

$$h_{12}(1,1;0,0) = \alpha, \quad h_{12}(0,0;0,0) = -\alpha,\tag{16}$$

but this breaks assumption (12) and a simple fix cannot be found, namely it is not sufficient to only edit the first rule, since if that were true, $P(1,1,1,1)$ would be $P(1,1,1)/\beta$ by the third rule, when in fact

$$\begin{aligned}P(1,1,1) &\propto \alpha^2(1 + \beta), \\ P(1,1,1,1) &\propto \alpha^2(\alpha^2(\beta^3 + 4\beta^2 + 6\beta + 2) + \alpha(\beta^4 + 5\beta^3 + 10\beta^2 + 8\beta + 2) \\ &\quad + \beta(\beta + 1)^2(\beta + 2)).\end{aligned}\tag{17}$$

So an algebra different from that in equation (14) should be constructed and shown to correspond to the steady state of this model. In fact, it is slightly unclear whether a matrix product solution even exists in this case.

I can follow chapter 2.4 of Rajewsky et al.^[21] model 2 to find an algebra by

having each lattice site have four possible states instead of two,

$$A = \begin{pmatrix} E \\ U \\ D \\ B \end{pmatrix}, \quad \bar{A} = \begin{pmatrix} \bar{E} \\ \bar{U} \\ \bar{D} \\ \bar{B} \end{pmatrix}, \quad (18)$$

where the second set of matrices are called auxiliary matrices. The reasoning here is that we combine the first two lattice sites into one lattice site that is allowed to have four different states, empty (E), up (U), down (D) and both (B). The "Hamiltonian" has to be changed as well, to

$$\begin{aligned} h_1(1,1) &= -h_1(4,1) = \alpha & h_1(2,2) &= -h_1(3,2) = 1 \\ h(9,9) &= -h(3,9) = 1 & & \\ h_L(3,3) &= h_L(4,4) = -h_L(1,3) = -h(2,4) = \beta. & & \end{aligned} \quad (19)$$

where h_1 and h_L are 4 times 4 matrices and h is a 16 times 16 matrix and the unmentioned matrix elements are equivalent to zero.

Regrettably the resulting algebra comprising 24 equations, four for both of the edges and 16 for the bulk, does not seem helpful. There is no general method of finding matrices that satisfy such an algebra or any given algebra. One known method is given in chapter III B of Vanicat^[22], but it is difficult to use when there are many matrices and it involves guessing an ansatz.

To make recursion relations from the equations for model 2 like was done for TASEP would necessitate being able to choose some of the matrices to be scalars and it seems to me that you can do that only for one of them. Furthermore at present it is not certain that this method of finding the algebras works, so you can consider this all a conjecture.

A simpler algebra than that for model 2 results from not caring about which one of the first two lattice sites a particle resides in. This is equivalent to the rate of particles going from the first site to the second site being infinite. This is yet another model for looking at the effects that boundaries might impose on the system.

It is possible to view model 2 as a model in a ring geometry, if you add a special lattice site that can hold L particles. Particles would enter this site at rate β from the end of the original lattice and exit to the beginning of the original lattice at rate α . This interpretation of the system would allow writing probabilities as traces instead of inner products, which simplifies the theory.

4.5 Mean Field Theory

In a mean field theory variables or some of them are replaced by their average values.

4.5.1 Model 1

For model 1

$$\begin{aligned}
\frac{\partial \langle n_1 \rangle}{\partial t} &= \alpha \langle 1 - n_1 \rangle - \langle n_1(1 - n_2) \rangle, \\
\frac{\partial \langle n_i \rangle}{\partial t} &= \langle n_{i-1}(1 - n_i) \rangle - \langle n_i(1 - n_{i+1}) \rangle, \\
\frac{\partial \langle n_L \rangle}{\partial t} &= \langle n_{L-1}(1 - n_L) \rangle - \beta \langle n_L \rangle.
\end{aligned} \tag{20}$$

While these sorts of equations are pretty standard, a way to read the first one is that the time derivative of the occupation number of the first lattice site is α times the probability that the first lattice site is empty minus the probability that the first lattice site is occupied and the second lattice site is empty. These terms actually are the particle flows into and out of site 1

The simplest mean-field approximation of equation (20) results in

$$\begin{aligned}
\frac{\partial \rho_1}{\partial t} &\approx \alpha(1 - \rho_1) - \rho_1(1 - \rho_2), \\
\frac{\partial \rho_i}{\partial t} &\approx \rho_{i-1}(1 - \rho_i) - \rho_i(1 - \rho_{i+1}), \\
\frac{\partial \rho_L}{\partial t} &\approx \rho_{L-1}(1 - \rho_L) - \beta \rho_L,
\end{aligned} \tag{21}$$

where $\rho_i = \langle n_i \rangle$. Solving (21) for the steady state where all the time derivatives equal zero, while remembering that current J is the same everywhere, results in

$$\begin{aligned}
\rho_1 &\approx 1 - J/\alpha, \\
\rho_i &\approx 1 - J/\rho_{i-1}, \\
\rho_L &\approx J/\beta.
\end{aligned} \tag{22}$$

Deep in the bulk of the system

$$\begin{aligned}
\rho_i &\approx 1 - J/\rho_i \Rightarrow \rho_{\pm}^2 - \rho_{\pm} + J \approx 0, \quad \text{and} \\
J_{\pm} &= \rho_{\pm}(1 - \rho_{\pm}),
\end{aligned} \tag{23}$$

where $\rho_{+(-)}$ is the density in the high (low) density phase and $J_{+(-)}$ is the current in the high (low) density phase

Solving ρ_{\pm} and J_{\pm} from (23) using $\rho_{+} = \rho_1$ and $\rho_{-} = \rho_L$ from (22) results in

$$\begin{aligned}\rho_{-} &= \alpha, & J_{-} &= \alpha(1 - \alpha), \\ \rho_{+} &= 1 - \beta, & J_{+} &= \beta(1 - \beta)\end{aligned}\tag{24}$$

For this model this basic mean field theory happens to give correctly the mean density and current as well as the phase diagram at the limit of an infinite system.

4.5.2 Model 2

For model 2

$$\begin{aligned}\frac{\partial \langle n_1 \rangle}{\partial t} &= \alpha \langle (1 - n_1)(1 - n_2) \rangle - \langle n_1(1 - n_2) \rangle \\ \frac{\partial \langle n_2 \rangle}{\partial t} &= \alpha \langle (1 - n_1)(1 - n_2) \rangle + \langle n_1(1 - n_2) \rangle - \langle n_2(1 - n_3) \rangle \\ \frac{\partial \langle n_i \rangle}{\partial t} &= \langle n_{i-1}(1 - n_i) \rangle - \langle n_i(1 - n_{i+1}) \rangle \\ \frac{\partial \langle n_L \rangle}{\partial t} &= \beta \langle n_L \rangle.\end{aligned}\tag{25}$$

Taking the mean field approximation, but keeping $\langle n_1 n_2 \rangle$ as C in a slight generalization of the basic mean field theory, results in

$$\begin{aligned}\frac{\partial \rho_1}{\partial t} &= \alpha(1 - \rho_1 - \rho_2 + C) - \rho_1 + C \\ \frac{\partial \rho_2}{\partial t} &\approx \alpha(1 - \rho_1 - \rho_2 + C) + \rho_1 - C - \rho_2(1 - \rho_3) \\ \frac{\partial C}{\partial t} &\approx \alpha(1 - \rho_1 - \rho_2 + C) - C(1 - \rho_3) \\ \frac{\partial \rho_i}{\partial t} &\approx \rho_{i-1}(1 - \rho_i) - \rho_i(1 - \rho_{i+1}) \\ \frac{\partial \rho_L}{\partial t} &\approx \beta \rho_L.\end{aligned}\tag{26}$$

Solving (26) for the steady state, while remembering that current J is the same everywhere except at the first cell where current is $J/2$, results in

$$\begin{aligned}\rho_1 &\approx \frac{J + \rho_2}{2} \\ \rho_2 &\approx 1 - \frac{J}{\alpha} \left(\frac{1 + \alpha}{2} \right) \\ C &\approx \rho_2/2 \\ \rho_i &\approx 1 - \frac{J}{\rho_{i-1}} \\ \rho_L &\approx J/\beta.\end{aligned}\tag{27}$$

Solving ρ_{\pm} and J_{\pm} from (23) using $\rho_+ = \rho_2$ and $\rho_- = \rho_L$ from (27) results in

$$\begin{aligned}\rho_- &= \frac{2\alpha}{1+\alpha}, & J_- &= \frac{2\alpha}{1+\alpha}\left(1 - \frac{2\alpha}{1+\alpha}\right), \\ \rho_+ &= 1 - \beta, & J_+ &= \beta(1 - \beta)\end{aligned}\tag{28}$$

Comparing the results for model 1 (24) and for model 2 (28), I infer that it might be a good idea to compare model 2 with model 1 with $\alpha_1 = 2\alpha_2/(1 + \alpha_2)$.

4.5.3 Model 3

Similarly for model 3

$$\begin{aligned}\frac{\partial \rho_1}{\partial t} &= \alpha(1 - \rho_1 - \rho_2 + C) + \alpha'(\rho_2 - C) - \rho_1 + C \\ \frac{\partial C}{\partial t} &= \alpha'(\rho_2 - C) - C(1 - \rho_3) \\ \frac{\partial \rho_i}{\partial t} &= \rho_{i-1}(1 - \rho_i) - \rho_i(1 - \rho_{i+1}) \\ \frac{\partial \rho_L}{\partial t} &= \rho_{L-1}(1 - \rho_L) - \beta\rho_L.\end{aligned}\tag{29}$$

Since finding the solution was a bit tricky and I had to use Mathematica to do so, I will elaborate the process here slightly. First solve equation (29) for $\rho_2(\alpha, \alpha', J)$, then invert it to $J(\alpha, \alpha', \rho_2)$, then, remembering that $\rho_2 = \rho_-$, solve $\rho_-^2 - \rho + J(\alpha, \alpha', \rho_-) = 0$ for ρ_- . This results in

$$\begin{aligned}\rho_- &= \alpha \frac{1 + \alpha'}{1 + \alpha}, & J_- &= \alpha \frac{1 + \alpha'}{1 + \alpha} \left(1 - \alpha \frac{1 + \alpha'}{1 + \alpha}\right) \\ \rho_+ &= 1 - \beta, & J_+ &= \beta(1 - \beta).\end{aligned}\tag{30}$$

4.6 Domain Wall Theory

The phase diagram of ASEP is understood in terms of domain wall theory^[23], which I shall now elucidate briefly. Since model 1 has a symmetry with a model where particles are fed in to the system at rate β from the right, travel to the left, and are removed from it with rate α at the left edge, it suffices to examine the region $\alpha \geq \beta$.

For model 1 if α and β are $\ll 1/L$, the system will look something like (000001111). The domain wall is at the spot where the holes end and the particles begin. If the fast process of particles jumping to the right is ignored, the evolution of the system can be described as the domain wall moving to the right at rate β and to the left at rate α . This results in a biased random walk of the domain wall to the right with drift velocity $V = \beta - \alpha$.

To make this a bit more precise and to include model 2 a bit of mathematics is

in order. Obviously the local densities $\rho(i,t)$ and currents $J(i,t)$ satisfy a continuity equation

$$\frac{d}{dt}\rho(i,t) = J(i-1,t) - J(i,t), \quad (31)$$

which in the continuum limit goes to

$$\frac{d}{dt}\rho(x,t) = -\frac{d}{dx}J(x,t), \quad (32)$$

that is solved by

$$\begin{aligned} \rho(x,t) &= \rho(x-vt), \\ v &= \frac{J_+ - J_-}{\rho_+ - \rho_-}. \end{aligned} \quad (33)$$

Domain wall drift velocity v changes sign at $J_+ = J_-$, which occurs at $\beta = \alpha$ for model 1 and at $\beta = 2\alpha/(1 + \alpha)$ for model 2. This change in sign of drift velocity at explains the discontinuous change in density when crossing the phase boundary between the low density and high density phases.

5 Results

The main results of this thesis are these figures. In most of them, exact numerical solutions are used. In some plots, those are compared with solutions of the corresponding (in the mean field theory sense, see chapters 4.5.2 and 4.5.2) model 1.

Figures 6 and 7 show what the current as a function of α and β is like for models 1 and 2 when $L = 20$. These can be compared with the $L \rightarrow \infty$ phase diagram of figure 5. Physically, it is evident that also for model 2 the maximal current in the limit $L \rightarrow \infty$ is $J = J_{max} = 1/4$. These plots seem rather different, which is surprising taking into account the similarities in all the other pictures comparing the models in this chapter.

In figures 8 to 10 the current through the system as a function of α is plotted for different system sizes for models 1 and 2 when $\beta = 1$. From these figures it is evident that the convergence towards $L \rightarrow \infty$ is quite similar for models 1 and 2 and that a system of size 64 already has a maximum current almost indistinguishable from $1/4$, the value for an infinite system. The plot for model 1 at large L has been produced using the analytical expression 1.

In figure 11 the current through the system is plotted as a function of system size for different α :s when $\beta = 1$. These figures reveal that a system of size 20 is not as hopelessly small as might be guessed.

In section 4.5.2 we defined a 'corresponding' model 1 of a given model 2 by using the mean field theory. Another way to define the correspondence is to use the current as the criterion, requiring models 1 and 2 to yield the same current at fixed β . This way the correspondence becomes dependent on L . The result is shown in figure 12. The dashed line represents the mean field solution $\alpha_1 = 2\alpha_2/(1 + \alpha_2)$. We see that the current does not converge to the mean field theoretical result, but the discrepancy does not seem to be bad.

Figure 13 shows the density profiles of models 1 and 2 when $\alpha_2 = \alpha_1/(2 - \alpha_1)$ in various parts of the phase diagram. Figures 14 to 15 similarly show the probability distributions of the number of particles at different parts of the lattice. These pictures show that setting $\alpha_2 = \alpha_1/(2 - \alpha_1)$ probably gives a reasonably good a correspondence between the models.

Figures 14 to 16 compare the probability distributions of the total density across different parts of the system and in different parts of the phase diagram. These comparisons show that already at this small system size the behavior in the corresponding systems 1 and 2 are very similar indeed. The differences between corresponding systems 1 and 2 are understandably largest near to the entry of the system.

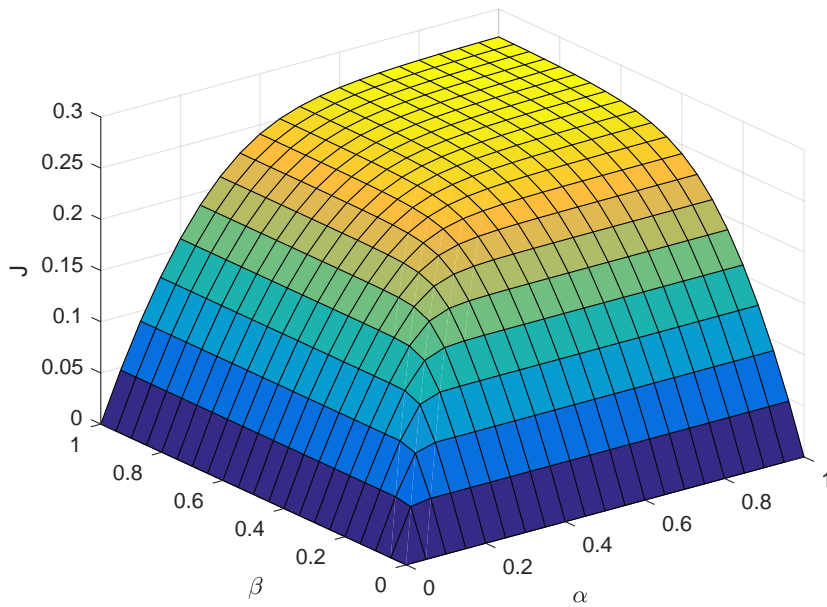


Figure 6. Current as a function of α and β for model 1 when $L = 20$.

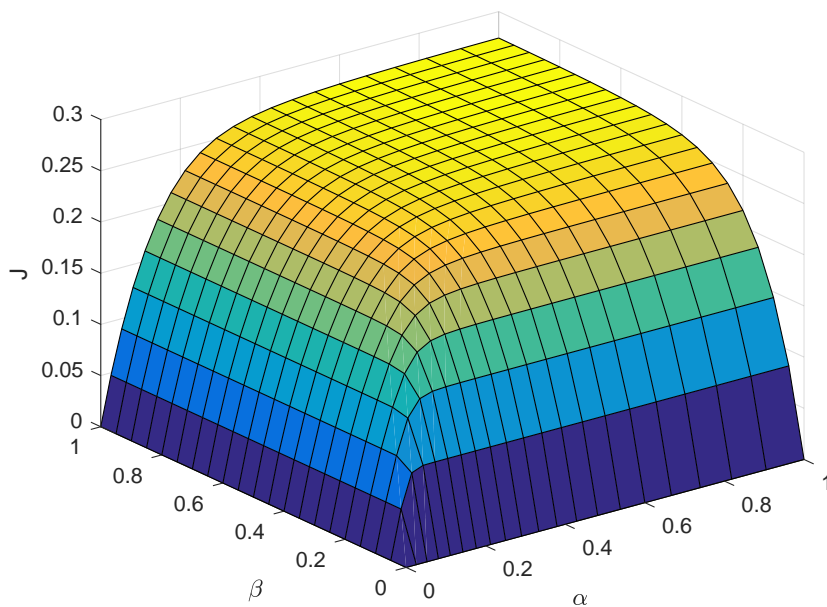


Figure 7. Current as a function of $\alpha/(2-\alpha)$ and β for model 2 when $L = 20$.

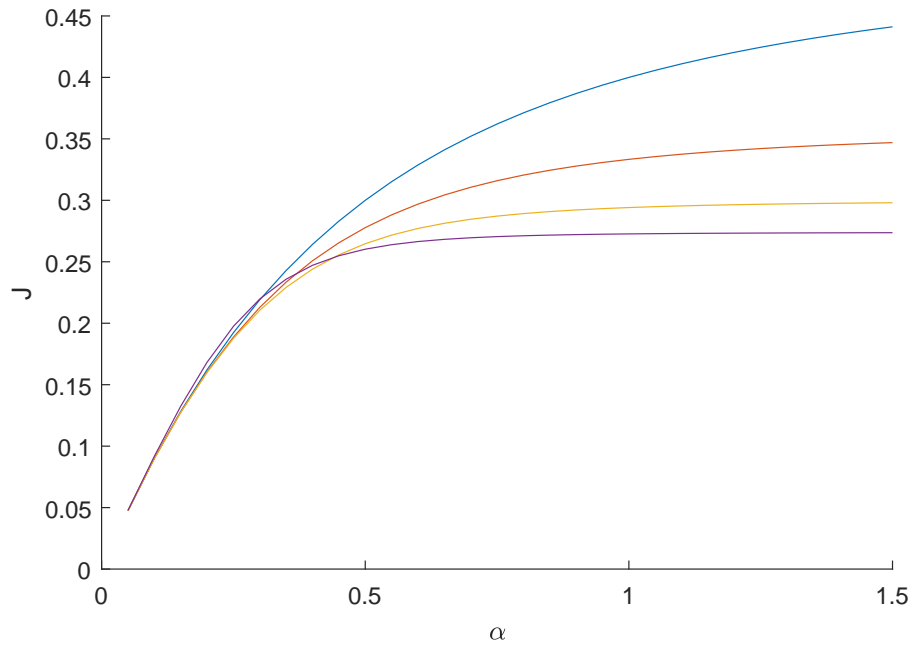


Figure 8. From top to bottom: current versus α for model 1 of sizes 2,4,8,16 when $\beta = 1$.

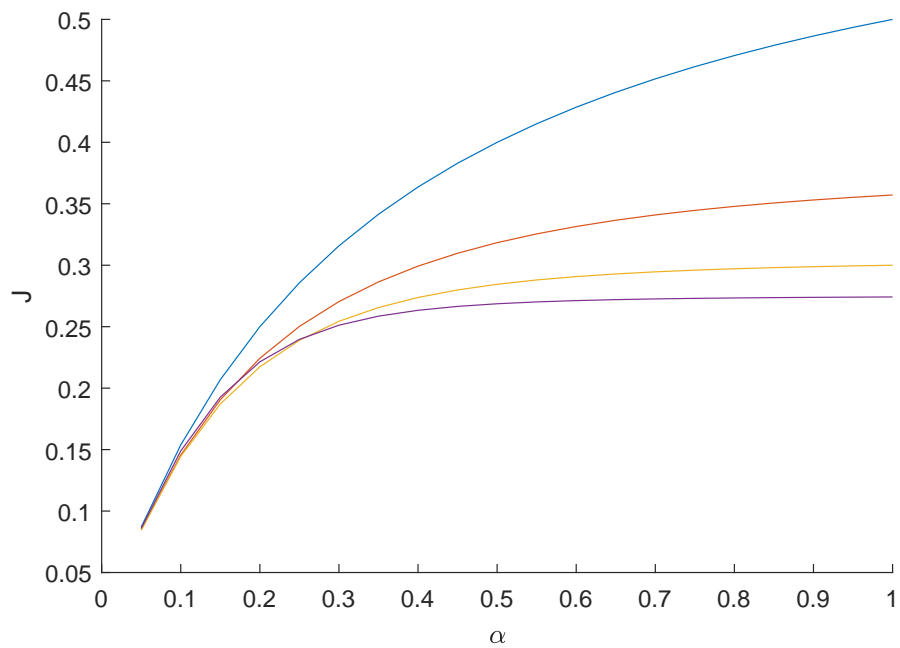


Figure 9. From top to bottom: current versus α for model 2 of sizes 2,4,8,16 when $\beta = 1$.

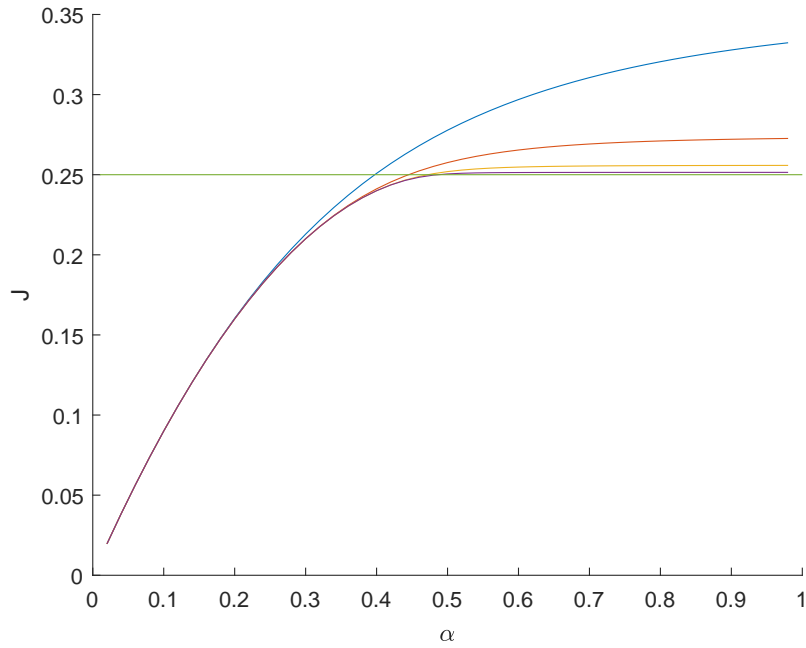


Figure 10. From bottom to top: current versus α for model 1 of sizes 4,16,64,256 when $\beta = 1$. The straight line is the high density phase current for an infinite system

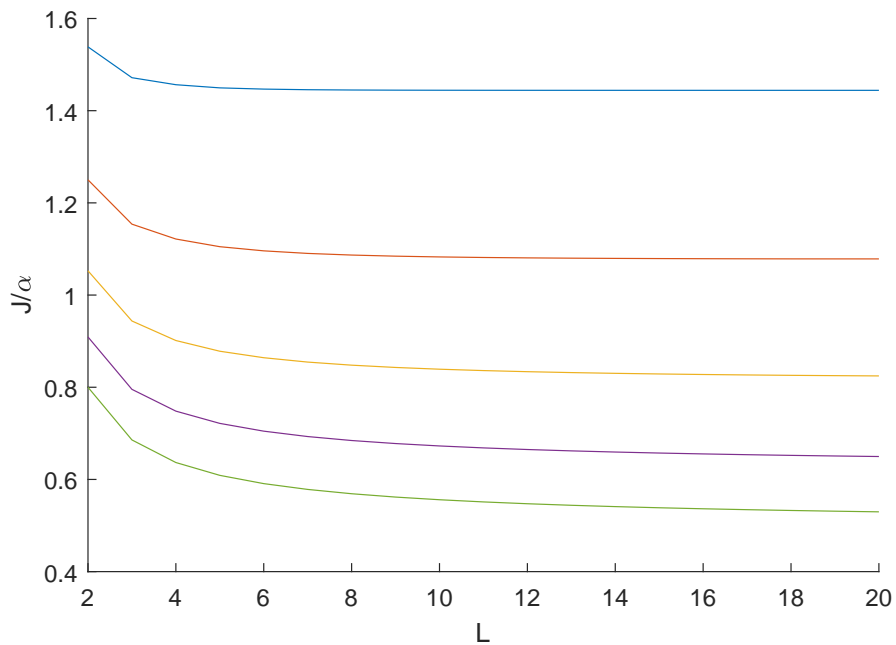


Figure 11. From top to bottom: current versus system size for model 2 when α is 0.1, 0.2, 0.3, 0.4, 0.5 when $\beta = 1$.

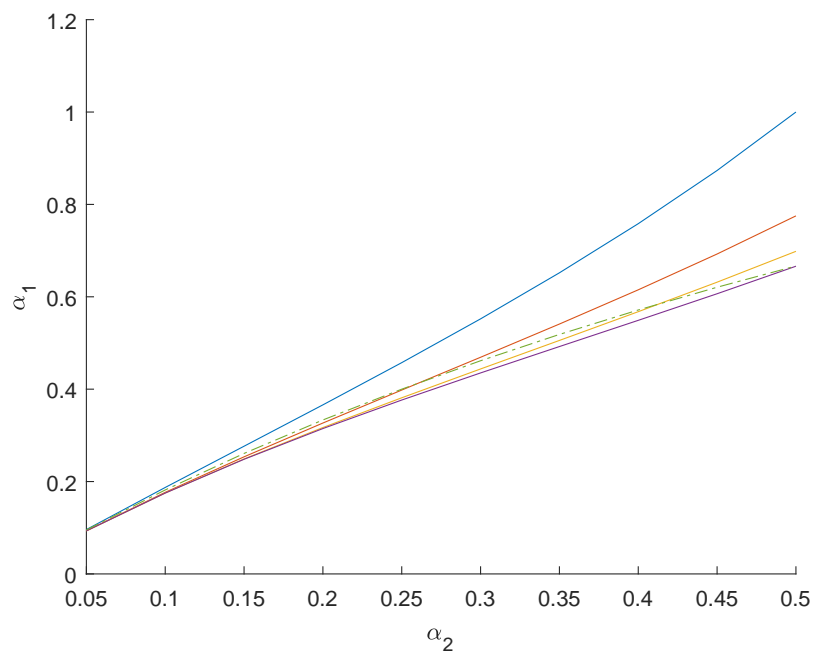


Figure 12. Solid lines from top to bottom: model 1 input rate α_1 that gives the same current as a given input rate α_2 for model 2 when L is 2,4,8,16 when $\beta = 1$. The dash-dotted line is $2\alpha_2/(\alpha_2 + 1)$, the mean field theoretical result.

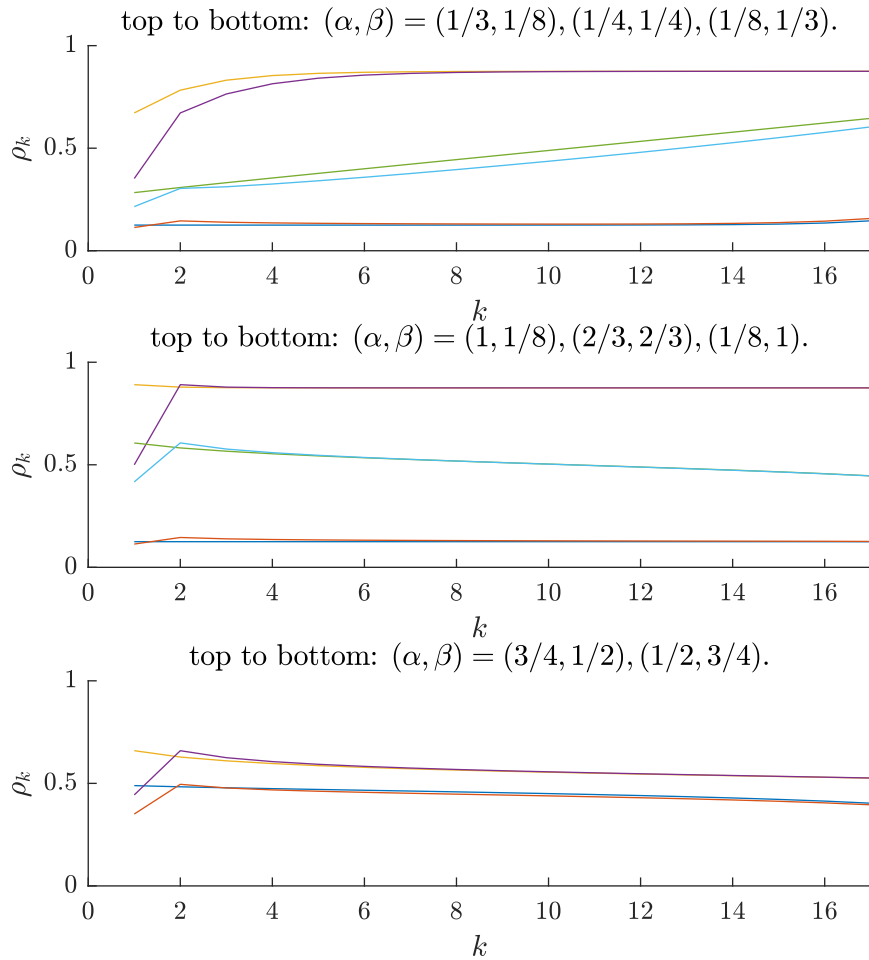


Figure 13. Density profiles for model 1 and a corresponding model 2 at various parts of the phase diagram when $L = 20$. In all pairs of lines, the one corresponding to model 2 is the one that has a larger difference in density between the first and second lattice points.

In the LD phase the models are not as similar, and this is because when α is small and β is large the number of particles in the system is likely to be even as seen in figure 14 for $\alpha = 1/4$. Even particle numbers are easily understood as a consequence of particles entering the system in pairs and staying close together relative to the distance between pairs of particles that is large due to small α , and leaving the system at a time proportional to their distance since β is large. As the system grows larger I would expect this effect to diminish at the right edge of the system due to increasing distance of particles in a pair.

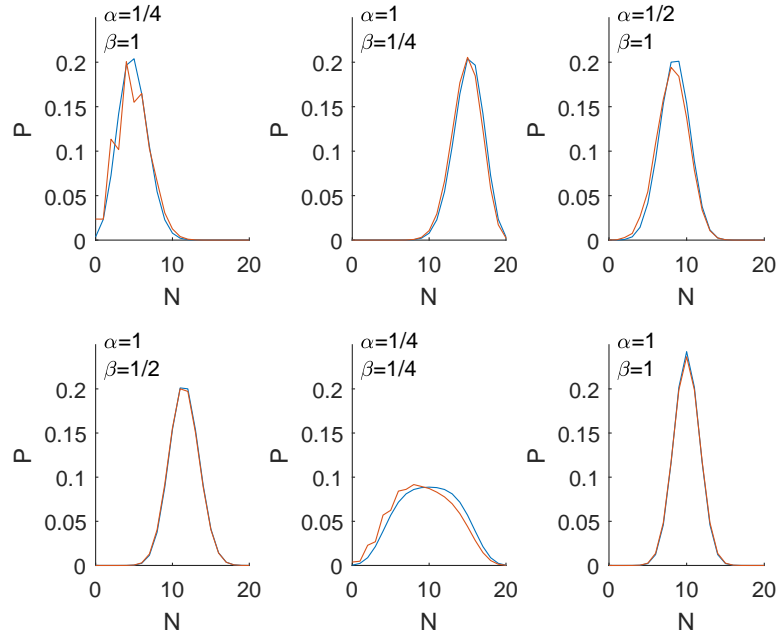


Figure 14. Probability distribution of the total density for $L = 20$. Model 1 in blue and the corresponding model 2 in red. The values of α are for model 1.

Figure 17 shows the probability distribution of the nearest neighbor correlation $\sum_i n_i n_{i+1}$ at all phases and phase boundaries. The high density phase has a peculiar shape resembling stairs.

In figure 19 the contours of the quantity $\xi = (\xi_\alpha^{-1} + \xi_\beta^{-1})^{-1} = \ln(J_+/J_-)$, called here the correlation length, are shown for model 1. This has been done previously in Kolomeisky et al.^[23]. The point of this figure is to show that as one nears the phase boundary, the correlation length increases without limit, so the effect of boundaries extends over the entire system at the coexistence line.

Density profiles for model 3 at various parts of the phase diagram are shown in figure 18. It seems that the density profile stays near to that of model 1 except when α is small and α_0 is a small portion of that. Even in that case the current stays near to that of the corresponding model 1.

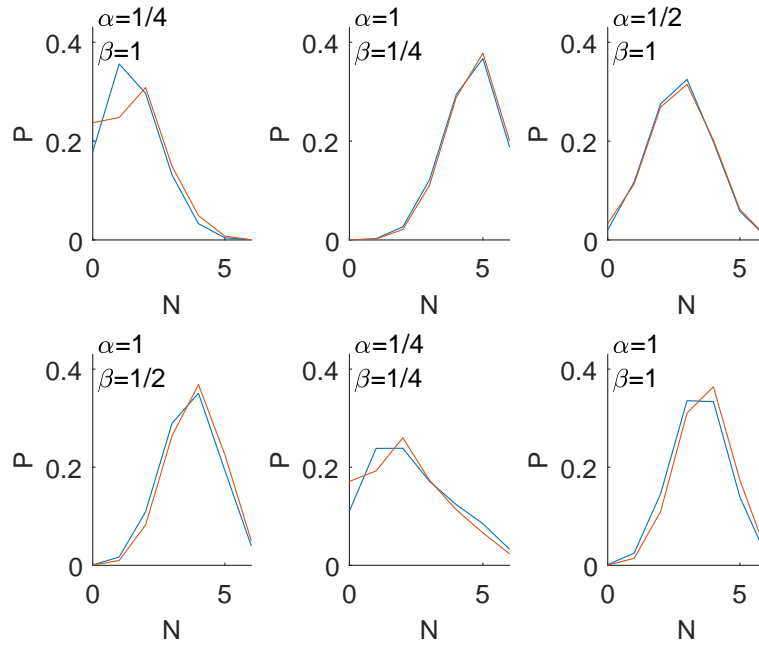


Figure 15. Probability distribution of the density at sites 2-7 for $L = 20$. Model 1 in blue and the corresponding model 2 in red.

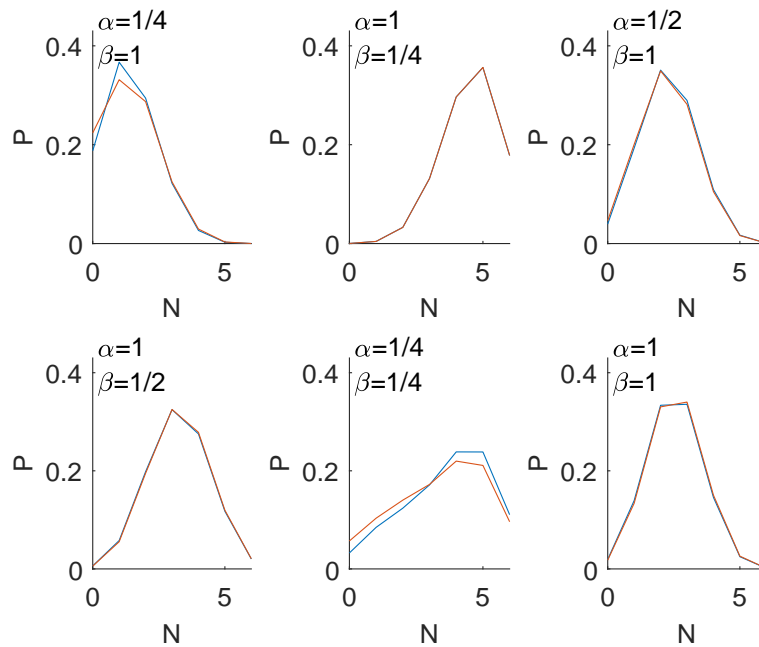


Figure 16. Probability distribution of the density at sites 10-15 for $L = 20$. Model 1 in blue and the corresponding model 2 in red.

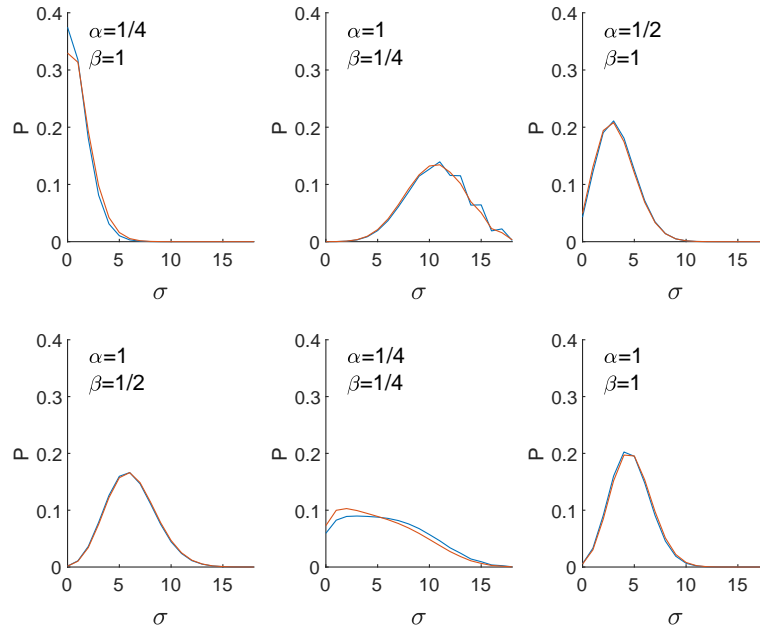


Figure 17. Probability distribution of $\sum_i n_i n_{i+1}$ for $L = 20$. Model 1 in blue and the corresponding model 2 in red. The values of α are for model 1.

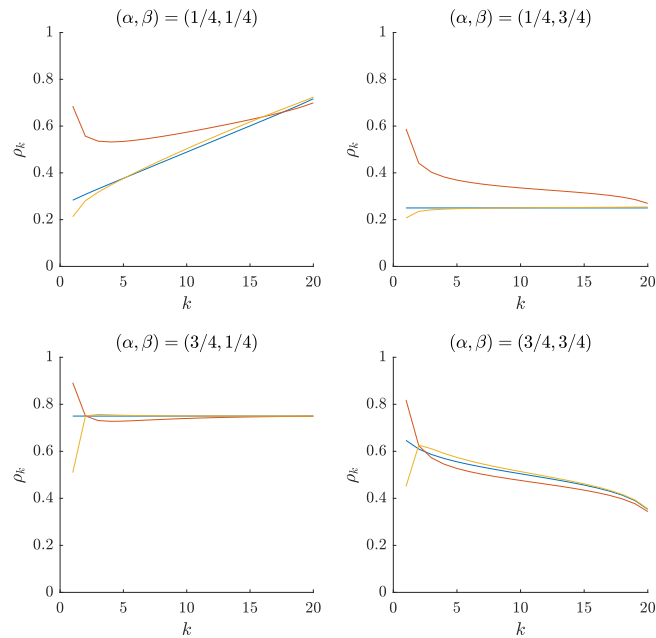


Figure 18. Density profiles for model 3. Red is for $\alpha_0 = \alpha/4$ and $\alpha_1 = (1 + 1/\alpha_0)\alpha - 1$. Blue is for $\alpha_0 = \alpha_1 = \alpha$, corresponding to model 1, and yellow is for $\alpha_1 = \alpha/4$

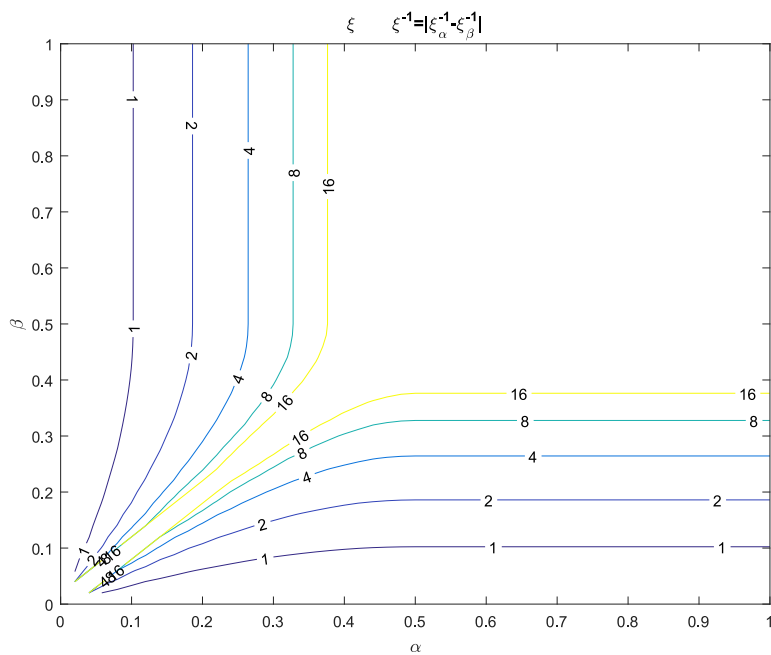


Figure 19. Correlation length ξ increases as the system nears a phase boundary. Picture courtesy of Juha Merikoski

6 Conclusion

The aim of this thesis was to study the boundary effects in TASEP. The central result is the finding that the mean field theory works decently, at least when it comes to density profiles and current, for most of the boundary effects considered, and already for quite small system sizes.

Calculations done in chapters 4.5 and 4.6 showed that a model 1 might correspond to a model 2 with $\alpha = 2\alpha' / (\alpha' + 1)$ and to a model 3 with $\alpha = \alpha_0(1 + \alpha_1) / (1 + \alpha_0)$. Figures 13 to 16 show that the correspondence is good for the density profile of model 2, especially outside the LD phase. For model 3 the density profile was also quite similar to that of model 1 outside the LD phase, but in the LD phase having a small α_0 results in an entirely different density profile from that of the corresponding model 1. In all the cases the correspondence for currents is pretty good.

Finally I shall suggest some ideas for further work. The models could be simulated for larger systems ($L = 100 \dots 1000$) using Monte Carlo simulation. Fluctuations of current could be studied, along with time correlations. Analytic solutions could be attempted since there are multiple frameworks for doing that, although it seems daunting. Some other models for boundary effects could also be considered.

References

- [1] Lars Onsager. Reciprocal relations in irreversible processes. i. *Phys. Rev.*, 37: 405–426, Feb 1931. doi: 10.1103/PhysRev.37.405. URL <https://link.aps.org/doi/10.1103/PhysRev.37.405>.
- [2] Ryogo Kubo. Statistical-mechanical theory of irreversible processes. i. general theory and simple applications to magnetic and conduction problems. *Journal of the Physical Society of Japan*, 12(6):570–586, 1957. doi: 10.1143/JPSJ.12.570. URL <https://doi.org/10.1143/JPSJ.12.570>.
- [3] B Schmittmann and R.K.P Zia. Driven diffusive systems. an introduction and recent developments. *Physics Reports*, 301(1-3):45–64, 1998. doi: [http://dx.doi.org/10.1016/S0370-1573\(98\)00005-2](http://dx.doi.org/10.1016/S0370-1573(98)00005-2). URL <http://www.sciencedirect.com/science/article/pii/S0370157398000052>.
- [4] Carolyn T. MacDonald, Julian H. Gibbs, and Allen C. Pipkin. Kinetics of biopolymerization on nucleic acid templates. *Biopolymers*, 6(1):1–25. doi: 10.1002/bip.1968.360060102. URL <https://onlinelibrary.wiley.com/doi/abs/10.1002/bip.1968.360060102>.
- [5] T Chou, K Mallick, and R K P Zia. Non-equilibrium statistical mechanics: from a paradigmatic model to biological transport. *Reports on Progress in Physics*, 74(11):116601, 2011. URL <http://stacks.iop.org/0034-4885/74/i=11/a=116601>.
- [6] Debashish Chowdhury, Ludger Santen, and Andreas Schadschneider. Statistical physics of vehicular traffic and some related systems. *Physics Reports*, 329(4):199 – 329, 2000. ISSN 0370-1573. doi: [https://doi.org/10.1016/S0370-1573\(99\)00117-9](https://doi.org/10.1016/S0370-1573(99)00117-9). URL <http://www.sciencedirect.com/science/article/pii/S0370157399001179>.
- [7] Kai Nagel and Michael Schreckenberg. A cellular automaton model for freeway traffic. *J. Phys. I France*, 2(12):2221–2229, 1992. doi: 10.1051/jp1:1992277. URL <https://doi.org/10.1051/jp1:1992277>.
- [8] G. M. Schütz. Experimental Realizations of Integrable Reaction-Diffusion Processes in Biological and Chemical Systems. *eprint arXiv:cond-mat/9601082*, January 1996.

- [9] B. Widom, J. L. Viovy, and A. D. Defontaines. Repton model of gel electrophoresis and diffusion. *J. Phys. I France*, 1(12):1759–1784, 1991. doi: 10.1051/jp1:1991239. URL <https://doi.org/10.1051/jp1:1991239>.
- [10] Shu chao Cao, Wei guo Song, Xiao dong Liu, and Nan Mu. Simulation of pedestrian evacuation in a room under fire emergency. *Procedia Engineering*, 71:403 – 409, 2014. ISSN 1877-7058. doi: <https://doi.org/10.1016/j.proeng.2014.04.058>. URL <http://www.sciencedirect.com/science/article/pii/S1877705814004767>. 2013 International Conference on Performance-based Fire and Fire Protection Engineering, Wuhan (ICPFPE 2013).
- [11] Volker Kukla, Jan Kornatowski, Dirk Demuth, Irina Girnus, Harry Pfeifer, Lovat V. C. Rees, Stefan Schunk, Klaus K. Unger, and Jörg Kärger. Nmr studies of single-file diffusion in unidimensional channel zeolites. *Science*, 272(5262):702–704, 1996. ISSN 00368075, 10959203. URL <http://www.jstor.org/stable/2889439>.
- [12] M. Myllys, J. Maunuksela, M. Alava, T. Ala-Nissila, J. Merikoski, and J. Timonen. Kinetic roughening in slow combustion of paper. *Phys. Rev. E*, 64:036101, Aug 2001. doi: 10.1103/PhysRevE.64.036101. URL <https://link.aps.org/doi/10.1103/PhysRevE.64.036101>.
- [13] B. Derrida, E. Domany, and D. Mukamel. An exact solution of a one-dimensional asymmetric exclusion model with open boundaries. *Journal of Statistical Physics*, 69(3):667–687, Nov 1992. ISSN 1572-9613. doi: 10.1007/BF01050430. URL <https://doi.org/10.1007/BF01050430>.
- [14] B. Derrida and M.R. Evans. Exact correlation functions in an asymmetric exclusion model with open boundaries. *J. Phys. I France*, 3(2):311–322, 1993. doi: 10.1051/jp1:1993132. URL <https://doi.org/10.1051/jp1:1993132>.
- [15] B Derrida, M R Evans, V Hakim, and V Pasquier. Exact solution of a 1d asymmetric exclusion model using a matrix formulation. *Journal of Physics A: Mathematical and General*, 26(7):1493, 1993. URL <http://stacks.iop.org/0305-4470/26/i=7/a=011>.
- [16] R A Blythe and M R Evans. Nonequilibrium steady states of matrix-product form: a solver’s guide. *Journal of Physics A: Mathematical and Theoretical*, 40(46):R333, 2007. URL <http://stacks.iop.org/1751-8121/40/i=46/a=R01>.
- [17] Alexandre Lazarescu and Kirone Mallick. An exact formula for the statistics of the current in the tasep with open boundaries. *Journal of Physics A: Mathematical and Theoretical*, 44(31):315001, 2011. URL <http://stacks.iop.org/1751-8121/44/i=31/a=315001>.

- [18] A. Lazarescu. The physicist's companion to current fluctuations: one-dimensional bulk-driven lattice gases. *Journal of Physics A Mathematical General*, 48:503001, December 2015. doi: 10.1088/1751-8113/48/50/503001.
- [19] M.L. Bellac, F. Mortessagne, and G.G. Batrouni. *Equilibrium and Non-Equilibrium Statistical Thermodynamics*. Cambridge University Press, 2004. ISBN 9780521821438. URL <https://books.google.fi/books?id=LZcdi4uzaWIC>.
- [20] Daniel T Gillespie. A general method for numerically simulating the stochastic time evolution of coupled chemical reactions. *Journal of Computational Physics*, 22(4):403 – 434, 1976. ISSN 0021-9991. doi: [https://doi.org/10.1016/0021-9991\(76\)90041-3](https://doi.org/10.1016/0021-9991(76)90041-3). URL <http://www.sciencedirect.com/science/article/pii/0021999176900413>.
- [21] N. Rajewsky, L. Santen, A. Schadschneider, and M. Schreckenberg. The asymmetric exclusion process: Comparison of update procedures. *Journal of Statistical Physics*, 92(1):151–194, Jul 1998. ISSN 1572-9613. doi: 10.1023/A:1023047703307. URL <https://doi.org/10.1023/A:1023047703307>.
- [22] M. Vanicat. An integrabilist approach of out-of-equilibrium statistical physics models. August 2017. URL <https://arxiv.org/abs/1708.02440>.
- [23] Anatoly B Kolomeisky, Gunter M Schütz, Eugene B Kolomeisky, and Joseph P Straley. Phase diagram of one-dimensional driven lattice gases with open boundaries. *Journal of Physics A: Mathematical and General*, 31(33):6911, 1998. URL <http://stacks.iop.org/0305-4470/31/i=33/a=003>.

